Lycium barbarum polysaccharides attenuate cardiovascular oxidative stress injury by enhancing the Keap1/Nrf2 signaling pathway in exhaustive exercise rats

XIAOHUI HU[1,2*], LE MU[1*], LINGQIN ZHU[2], XIAOYU CHANG[2], LIHONG NIE[1], LI WANG[3] and GUANGHUA LI[1,2]

[1]School of Basic Medical Sciences, [2]School of Public Health and Management, Ningxia Medical University; [3]Department of General Practice, General Hospital of Ningxia Medical University, Yinchuan, Ningxia 750004, P.R. China

Received June 11, 2020; Accepted March 12, 2021

DOI: 10.3892/mmr.2021.12282

Abstract. Moderate exercise is beneficial to physical and mental health. When the amount of exercise and exercise intensity exceeds a certain limit and reaches the state of exhaustion, oxidative stress levels in the body increase, which can lead to oxidative stress-associated damage. *Lycium barbarum* polysaccharide (LBP) is one of the primary active ingredients extracted from wolfberry. Following exhausting exercise in rats, LBP supplements decrease damage to the myocardium and blood vessels, indicating that LBP exerts a protective effect on the cardiovascular system. The Kelch-like ECH-associated protein 1 (Keap1)/NF-E2-related factor 2 (Nrf2) anti-oxidative stress signaling pathway improves total oxidizing ability; anti-apoptosis and other aspects serve a vital role. In the present study, LBP intervention was performed *in vivo* and *in vitro* to observe its effect on the Keap1/Nrf2 pathway and oxidative stress-associated indicators in order to clarify its protective mechanism. For the *in vivo* experiments, 60 male Sprague-Dawley rats were randomly divided into normal control and aerobic, exhaustive and exhaustive exercise + LBP (200 mg/kg/day) groups. For the *in vitro* experiments, a rat thoracic aortic endothelial cell (RTAEC) oxidative stress model was established using angiotensin II (AngII) and divided into blank control, LBP (3,200 μg/ml), AngII ($1x10^{-4}$ mol/l) and AngII + LBP groups. For *in vitro* experiments, small interfering (si)RNA (50 nmol) was used to transfect RTAEC and induce gene silencing of Nrf2. ELISA, hematoxylin and eosin staining, TUNEL, immunofluorescence, western blotting, immunohistochemistry and reverse transcription-quantitative PCR were used to evaluate and verify the effect of LBP on oxidative stress indicators and the expression of Keap1/Nrf2 antioxidative stress signaling pathway. The *in vivo* experiments showed that LBP decreased the expression of serum malondialdehyde (MDA) and AngII, as well as apoptosis of blood vessels and cardiomyocytes and expression of TNF-α in rats following exhaustive exercise. Meanwhile, LBP enhanced expression of the Keap1/Nrf2 signaling pathway and downstream associated protein glutamyl-cysteine synthetase catalytic subunit (GCLC), quinone oxidoreductase 1 (NQO1) and glutamate-cysteine ligase modified subunit (GCLM) in the thoracic aorta and myocardium of rats following exhaustive exercise. In RTAEC *in vitro*, LBP decreased the expression of MDA and TNF-α in the supernatant, promoted the nuclear translocation of Nrf2 and increased expression levels of GCLC, NQO1 and GCLM. Following siNrf2 transfection into endothelial cells, the anti-inflammatory and antioxidant stress effects of LBP were decreased. LBP was found to enhance the expression of the Keap1/Nrf2 antioxidant stress signaling pathway in endothelial cells, decreasing oxidative stress and the inflammatory response. Moreover, LBP improved the antioxidant stress ability of endothelial cells and alleviated injury of myocardial vascular tissue, thereby protecting the cardiovascular system.

Correspondence to: Professor Guanghua Li, School of Basic Medical Sciences, Ningxia Medical University, 1160 Shengli Street, Yinchuan, Ningxia 750004, P.R. China
E-mail: ghlee0404@163.com

Professor Li Wang, Department of General Practice, General Hospital of Ningxia Medical University, 804 Shengli South Street, Yinchuan, Ningxia 750004, P.R. China
E-mail: gt2018243@sina.com

*Contributed equally

Key words: Lycium barbarum polysaccharide, oxidative stress, endothelial cells, Kelch-like ECH-associated protein 1/NF-E2-related factor 2, small interfering RNA

Introduction

Moderate exercise accelerates tissue metabolism, eliminates excessive free radicals and improves heart metabolic health and immune defense (1,2); however, the level of oxidative stress increases when the amount and intensity of exercise exceeds a certain limit (3,4). Studies have shown that high levels of oxidative stress in the body, such as other factors like high temperature, long-term high-intensity training, hypertension and hyperlipidemia are important risk factors

for endothelial cell dysfunction, which is a key event in the occurrence of cardiovascular disease (5-8). In the progress of vascular complications caused by diabetes, the regulation of endothelial function and related signaling pathways have been well studied (9). Therefore, improving the antioxidant stress function of endothelial cells and reducing the level of oxidative stress to prevent and delay the occurrence and development of cardiovascular injury and its complications has attracted the interest of the research community.

The Kelch-like ECH-associated protein 1 (Keap1)/NF-E2-related factor 2 (Nrf2) pathway serves a key role in improving total antioxidant capacity, anti-apoptosis and anti-tumor activity, anti-inflammatory response and neuroprotection (10-12). Nrf2 binds to cytoplasm Keap1 and exists in the cytoplasm in an inactive state. Due to the change of intracellular redox balance, Keap1 is inactivated by modification of cysteine residues and loses the ability to interact with Nrf2. The dissociated Nrf2 then shifts to the nucleus, dimerizes with small members of the Maf family and binds to the antioxidant response element (ARE), promoting the expression of Nrf2 target genes such as glutamyl cysteine synthetase catalytic subunit (GCLC), glutamate (GLU)-cysteine ligase modified subunit (GCLM) and quinone oxidoreductase 1 (NQO1). After the oxidative stress stimulation from the body and the outside world is released, Nrf2 returns to its initial level after a series of regulations (13-18).

Lycium barbarum polysaccharides (LBP) are extracted from Chinese wolfberry. LBP exhibits anti-inflammation, anti-oxidation, anti-apoptosis and immunomodulation activity, and can protect neurons and inhibit tumor growth (19-24). The aim of the present study was to investigate whether LBP enhances the expression of the Keap1/Nrf2 antioxidant stress signaling pathway in cardiovascular endothelial cells and improves antioxidant capacity in a cellular model and oxidative stress state, thus protecting the cardiovascular system.

For *in vivo* experiments, SD rats were randomly divided into four groups: Normal control group, aerobic exercise group, exhaustive exercise group, exhaustive exercise + LBP group. Following modeling, the myocardium and thoracic aorta of the rats were taken for follow-up experiments. ELISA, hematoxylin and eosin staining, TUNEL, immunofluorescence, western blotting, immunohistochemistry and reverse transcription-quantitative PCR (RT-qPCR) were used to explore the preliminary mechanism at the animal level. For *in vitro* experiments, RTAEC was used to prepare oxidative stress models using Ang II, and ELISA, hematoxylin and eosin staining, TUNEL, immunofluorescence, western blotting, immunohistochemistry and reverse transcription-quantitative PCR were used to further study the mechanism. At the same time, small interfering RNA transfection experiments were performed to verify the mechanism at the cellular level.

Materials and methods

Reagents. TNF-α (cat. no. AF7014), Keap1 (cat. no. AF5266), Nrf2 (cat. no. AF0639) and phosphorylated (p-)Nrf2 (p-Nrf2; cat. no. DF7519) were obtained from Affinity Biosciences. GCLM (cat. no. 14241-1-AP) and GCLC (cat. no. 12601-1-AP) were obtained from ProteinTech Group, Inc. NQO1 (cat. no. SC-376023) was obtained from Santa Cruz Biotechnology, Inc. Bax (cat. no. ab32503), Bcl-2 (cat. no. ab59348) and caspase-3 (cat. no. ab13847) were obtained from Abcam. Small interfering (si)RNA and fluorescent siRNA transfection kits (cat. nos. R10043.8 and R11077.2, respectively) and HiPerFect transfection reagent (cat. no. 301702) were obtained from Ruibo Bio-Technology Co., Ltd. ELISA kits for glutathione (GSH; cat. no. CEA294Ge), malondialdehyde (MDA; cat. no. CEA294Ge), peroxidation catalase (CAT; cat. no. SEC418Ra) and angiotensin (Ang)II (cat. no. CEA005Ge) were obtained from Cloud-Clone Corp. Total antioxidation capacity (T-AOC) ELISA kit (cat. no. SU-BN31087) was obtained from Jiangsu Jingmei Biotechnology Co., Ltd. Reverse transcription-quantitative (RT-q)PCR Primer was obtained from Sangon Biotech Co., Ltd. eBioscience™ Intracellular Fixation & Permeabilization Buffer Set (cat. no. 88-8824-00) was obtained from Thermo Fisher Scientific, Inc. LBP was obtained from Ningxia Qiyuan Pharmaceutical Co., Ltd. One-step TUNEL apoptosis *in situ* detection (cat. no. KGA7061) and BCA protein assay kits (cat. no. KGPBCA) were obtained from Nanjing KeyGen Biotech Co., Ltd. Human AngII (cat. no. 4474-91-3) was obtained from Merck KGaA.

Assessment of oxidative stress. When the body is stimulated by the external environment (exercise), it activates the renin-Ang system in the body. The expression of AngII and oxidative stress rise, which is manifested by increased levels of oxidase and decrease levels of antioxidant enzymes. SOD and CAT regulate oxidative stress and free radicals. When the level of oxidative stress increases, MDA can be used as an indicator of lipid peroxidation. T-AOC reflects the degree of oxidative stress and total levels of all antioxidants. Therefore, the oxidative stress state can be reflected by measuring the levels of AngII, oxidase and antioxidant enzymes in serum (25,26). ELISA kits were used according to the manufacturer's protocols and used to detect the levels of AngII in rat serum, as well of those in GSH, MDA, CAT and T-AOC in rat serum and cell culture medium using a microplate reader to measure the optical density value and plot a standard curve to calculate the concentration and reflect oxidative stress level.

Research animals and cells. Animal experiments were approved by the Animal Ethics and Use Committee of Ningxia Medical University (Yinchuan, China) in accordance with the guidelines of the Council of the Chinese Physiological Society. A total of 60 healthy male Sprague-Dawley rats (6-8 weeks, 180-220 g; Experimental Animal Center of Ningxia Medical University) are kept at room temperature (18-22˚C), humidity 45-65%, with a 12 h light/dark cycle and had free access to food and water. Rat thoracic aortic endothelial cells (RTAECs) were purchased from Shanghai Saiqi Biological Engineering Co., Ltd.

Preparation of experimental model in vivo. Rats were divided into normal control (Control), aerobic exercise (AE), exhaustive exercise (EX) and EX + LBP groups (n=15/group). Control rats did not do any exercise, while the other three groups swam for 1 h. The period of swimming training was 5 weeks; adaptive swimming training was performed in the first week (10 min on day 1, increasing by 10 min/day to 60 min on day 6, followed by rest on day 7). For the remaining 4 weeks,

Table I. Primer sequences.

Gene	Forward, 5'→3'	Reverse, 5'→3'
TNF-α	GCATGATCCGAGATGTGGAACTGG	CGCCACGAGCAGGAATGAGAAG
IL-1β	ATCTCACAGCAGCATCTCGACAAG	CACACTAGCAGGTCGTCATCATCC
IL-6	AGGAGTGGCTAAGGACCAAGACC	TGCCGAGTAGACCTCATAGTGACC
Keap1	TGCTCAACCGCTTGCTGTATGC	TCATCCGCCACTCATTCCTCTCC
Nrf2	GCCTTCCTCTGCTGCCATTAGTC	TCATTGAACTCCACCGTGCCTTC
NQO1	AGAAGCGTCTGGAGACTGTCTGG	GATCTGGTTGTCGGCTGGAATGG
GCLC	GCACATCTACCACGCAGTCAAGG	TCAAGAACATCGCCGCCATTCAG
GCLM	CTGGACTCTGTCATCATGGCTTCC	TCCGAGGTGCCTATAGCAACAATC
β-actin	CACCCGCGAGTACAACCTTC	CCCATACCCACCATCACACC

Keap1, Kelch-like ECH-associated protein 1; Nrf2, NF-E2-related factor 2; NQO1, quinone oxidoreductase 1; GCLC, glutamyl-cysteine synthetase catalytic subunit; GCLM, glutamate-cysteine ligase modified subunit.

rats swam for 60 min/day, 5 days/week (rest on Tuesdays and Saturdays). After the final swimming session, rats in the EX and EX + LBP groups continued to swim to exhaustion, as previously described (27). Rats in the EX + LBP group were fed with LBP at a dose of 200 mg/kg/day (Ningxia Qiyuan Pharmaceutical Co., Ltd.) after exercise. Animals were anesthetized with 10% chloral hydrate (300 mg/kg). Hemostatic forceps were used to clamp the limbs; lack of resistance and pain reflex indicated that anesthesia was successful (absence of peritonitis following the use of 10% chloral hydrate). Blood (4-5 ml), thoracic aorta and myocardium samples were collected from rats under anesthesia with chloral hydrate. Following blood centrifugation (1,798 x g at 4˚C for 3 min), serum was collected and placed in a refrigerator at -80˚C. Part of the myocardium and blood vessels were fixed in 4% paraformaldehyde at room temperature for 24 h; the other part of the heart and blood vessels were placed in a refrigerator at -80˚C. The specimens were used for subsequent experiments.

Preparation of experimental model in vitro. RTAECs were cultured in DMEM (Thermo Fisher Scientific, Inc.) with 10% fetal bovine serum (Clark Bioscience; cat. no. FB35015). All cells in the experiment were cultured at 37˚C, and 5% CO_2 and the subsequent test performed when the cell confluence was 70-80%. A RTAEC oxidative stress model was established to study the mechanism of LBP alleviating oxidative stress injury using the following groups: i) Blank control, cells cultured in fresh culture medium (37˚C, 5% CO_2); ii) LBP, cells cultured in medium containing LBP (3,200 μg/ml) for 2 h, then fresh medium for 24 h; iii) AngII, cells cultured in fresh medium for 2 h, then medium containing AngII ($1x10^{-6}$ mol/l) for 24 h; iv) AngII + LBP, cells cultured in medium containing LBP for 2 h, then medium containing AngII for 24 h. siRNA (50 nmol) was transfected with endothelial cells with assistance in HiPerfect. Specific steps are as follows: i) A single cell suspension ~$1x10^5$/ml was inoculated into a 6-well plate, 1 ml per well, then 4 ml of complete medium added per well, and then placed in the incubator for 24 h. ii) The siRNA stock solution was diluted according to the manufacturer's instructions; 120 μl of the serum-free-free-free medium was added together with 5 μl of 20 μmol siRNA stock solution. iii) HiPerfect (12 μl) was slowly added to the liquid prepared in step ii, and allowed to stand for 15 min, to form a transfection complex. iv) The culture solution was discarded, and 1,863 μl of non-double anti-medium added, and then the composite from step iii slowly added. v) For subsequent related experiments, siRNA transfection was performed using the following groups: i) Blank control, as aforementioned; ii) AngII, as aforementioned; iii) AngII + LBP, as aforementioned; iv) si non-specific control (siNC), siNC was transfected into cells using HiPerFect for 24 h; v) siNC + AngII + LBP, siNC was transfected into cells using HiPerFect for 24 h, then cells were cultured in medium containing LBP for 2 h, then for 24 h in medium containing AngII; vi) siRNA, siRNA was transfected into cells using HiPerFect for 24 h; vii) siRNA + AngII + LBP, siRNA was transfected into cells using HiPerFect for 24 h, then cells were cultured in medium containing LBP for 2 h, then for 24 h in medium containing AngII.

ELISA. Under anesthesia with chloral hydrate, the rat chest was opened and 3-5 ml blood was removed from the left ventricle with the tip of a 5 ml syringe to prevent hemolysis. Samples were transferred to a 15 ml centrifuge tube. After 30 min, samples were centrifuged at 4˚C, 5,035 x g. After 3min, the serum was taken and stored at -80˚C for follow-up experiments. Cell supernatant was collected, centrifuged at 4˚C, 5,035 x g for 3 min and stored at -80˚C for testing. Standards and samples were loaded into the enzyme plate, followed by incubation at 37˚C for 1 h. After washing, the substrate solution was loaded into the plate, followed by incubation at 37˚C in the dark for 15 min. The absorbance at 450 nm was measured after stop solution was loaded into the plate and the concentration of the sample was calculated.

Hematoxylin and eosin staining. Rat thoracic aorta and myocardium were fixed in 4% paraformaldehyde at room temperature for 24 h, paraffin-embedded, sectioned at 3 μm, dewaxed at 60˚C for 6-8 h, then placed at room temperature and dehydrated (2 min, 95% alcohol 1 min, 90% alcohol 1 min, 80% alcohol 1 min, 75% alcohol 13 min and 50% alcohol 1 min. Sections were stained in hematoxylin for 5 min at room temperature and eosin for 2-3 min at room temperature. The

sections were dehydrated with a graded series of alcohol and cleared in xylene, mounted neutral dried at room temperature before being observed under an inverted light microscope (magnification, x400).

TUNEL staining. The rat thoracic aorta and myocardium were sectioned at 3 μm, deparaffinized in xylene (20 min), and dehydrated with an ethanol gradient. The dehydration sequence and time were absolute ethanol I and II each for 2 min, 95% alcohol immersion for 1 min, 90% alcohol immersion for 1 min, 80% alcohol immersion for 1 min, 75% alcohol immersion for 1 min, and 50% alcohol immersion for 1 min. then add proteinase K working solution, DNaseI reaction solution, TdT enzyme reaction solution and Streptomyces dropwise Avidin-TRITC-labeled working solution were added and the sections placed in a 37˚C incubator for 30 min. DAPI (catalog number S2110; Beijing Solarbio Science & Technology Co., Ltd.) was added dropwise and observed under an inverted fluorescence microscope (magnification, x400).

Immunofluorescence. Rat thoracic aorta and myocardium were paraffin-embedded, dewaxed with xylene, dehydrated with alcohol gradient as aforementioned. Antigens were retrieved at 100˚C for 10 min and the sections permeated and blocked with normal goat serum (1:50) at 37˚C for 1 h. The sections were incubated with primary antibodies (Bax, 1:100; Bcl-2 and 1:100 and caspase-3, 1:50) at 4˚C overnight, followed by incubation with the corresponding horseradish enzyme-labeled goat anti-rabbit IgG (H+L) (cat. no. A21020; Abbkine Scientific Co., Ltd.; 1:50) and horseradish enzyme-labeled goat anti-mouse IgG (H+L) (cat. no. A21010; Abbkine Scientific Co., Ltd.; 1:50) at 37˚C for 1 h and DAPI stock solution in the dark for 10 min at room temperature and observed under an inverted fluorescence microscope (magnification, x400).

RTAEC single-cell suspensions were seeded into 24-well plates. When the cells reached 80% confluence, they were fixed with 4% paraformaldehyde for 30 min, 0.2% Triton X-100 and placed in a 37˚C incubator for 30 min (to improve the permeability of the cell membrane) and the serum was blocked with goat serum (OriGene Technologies, Inc.). After incubating with the primary antibody (Nrf2, 1:100 and GCLM, 1:50) at 4˚C overnight, the cells were incubated with the corresponding secondary antibody (1:50, 1 h) and DAPI stock solution for 10 min at room temperature in the dark and observed under an inverted fluorescence microscope (magnification, x400).

Western blotting. Rat thoracic aorta and myocardium tissue were lysed in lysis buffer (Nanjing KeyGen Biotech Co., Ltd.) containing 0.1% protease inhibitor, 1% phosphatase inhibitor and 1% phenylmethylsulfonyl fluoride followed by separation via SDS-PAGE (8%). Protein (50 μg) was loaded in each lane and transferred to PVDF membranes. After blocking with 5% skimmed milk at room temperature for 1 h, the membranes were probed with TNF-α (1:500), Keap1 (1:1,000), Nrf2 (1:700), NQO1 (1:800), GCLM (1:700), GCLC (1:2,000), β-actin (1:1,000) and GAPDH (1:5,000) antibodies at 4˚C overnight, washed Tween20 (1:1,000) and followed by incubation (3 times at room temperature, 15 min each time) with the corresponding secondary antibody (Goat anti-rabbit or goat anti-mouse; 1:5,000). The visualisation reagent was Drop ECL (Affinity Biosciences. USA) and the target bands were quantified by ImageJ 180 software (National Institutes of Health).

Immunohistochemistry. Tissues were paraffin-embedded, dewaxed in xylene, dehydrated with alcohol gradient, repaired by high temperature antigen and serum-blocked, as aforementioned, then incubated with TNF-α (1:100), Keap1 (1:100), Nrf2 (1:100), NQO1 (1:50), GCLM (1:150) and GCLC (1:100) primary antibodies at 4˚C overnight and reheated at 37˚C for 1-2 h the next day. Reaction enhancement solution (OriGene Technologies, Inc.) was added to the tissue sections, which were placed in a humidified box for 20 min at 37˚C. Universal two-step kit (mouse/rabbit enhanced polymer method detection system) was added and incubated at 37˚C for 1 h, followed by DAB color development (1 ml). Sections were washed in deionized water for 3-5 min, hematoxylin staining stock added to stain the nucleus for 2 min (room temperature) and washed 3 times in deionized water for 5 min each. The sections were differentiated in 0.5% 75% alcohol and concentrated hydrochloric acid for 5 sec, washed 3 times in water, each time for 5 min. Following washing, the sections were dehydrated 50, 75, 80, 90 and 95% ethanol, then anhydrous I and anhydrous ethanol II each for 30 sec. After transfer to xylene for 2-3 min, the sections were mounted in neutral resin. The positive results were observed using a light microscope (magnification, x400) and the results were analyzed using ImageJ v180 (National Institutes of Health).

Flow cytometry. Flow cytometry was performed to detect intracellular TNF-α antigen. Cells cultured at 70-80% confluence were trypsinized to make a single cell suspension and centrifuged at 200 x g at 4˚C 5 min. Following centrifugation, the cells were washed with 1 ml PBS, transferred to a 1.5ml EP tube, and diluted so that the number of cells per ml was $1x10^6$ cells Permeation solution was added to increase the cell permeability to ensure fluorescent labelled TNF-α antibody entered the cell and combined with the intracellular antigen. Antibody directly coupled to the intracellular antigen was added for 1 h and permeation solution was added to promote binding of antigen and antibody before centrifugation at 200 x g at 4˚C 5 min. Supernatant was discarded and expression levels of TNF-α in the cells were detected by flow cytometry with PBS and PE staining. A total of 50,000 cells was collected at an excitation wavelength of 488-561 nm. The number of TNF-α-positive cells was detected at 578 nm. Finally, the percentage of positive cells in the total number of cells was calculated as the expression level of TNF-α. Each experiment was repeated 6 times independently. GraphPad prim6 (GraphPad Software, Inc.) was used for statistical analysis.

Cell transfection. Before transfection, the cells need to grow well, and the cells need to pass resuscitation, passage, growth and fusion to the experimental state. siNrf2 was purchased from Guangzhou Ruibo Biotechnology Co., Ltd. HiPerFect was used to transfect siNrf2 (50 nmol) into endothelial cells. A single-cell suspension was prepared according to the method of cell passage, and cells were counted with an automatic cell counter. Cells ($1x10^5$ cells/ml) were inoculated into a 6-well plate and incubated at 37˚C for 24 h. siRNA stock solution was diluted according to the manufacturer's instructions the next

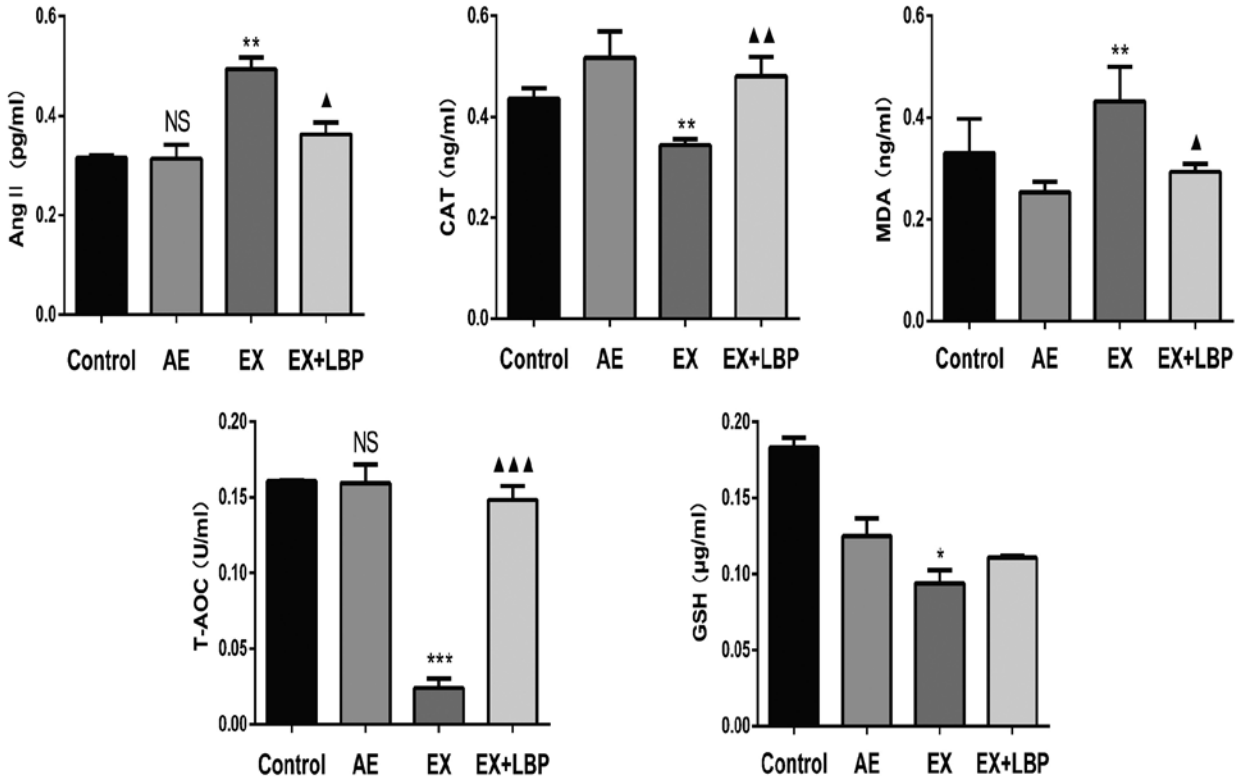

Figure 1. Effects of LBP and EX on serum AngII, CAT, MDA, T-AOC and GSH expression levels. *P<0.05, **P<0.01, ***P<0.001 vs. AE; ▲P<0.05, ▲▲P<0.01, ▲▲▲P<0.001 vs. EX. LBP, *Lycium barbarum* polysaccharide; AngII, angiotensin II; CAT, catalase; MDA, malonaldehyde; T-AOC, total antioxidation capacity; GSH, glutathione; AE, aerobic exercise; EX, exhaustive exercise; NS, no significance.

day. A total of 120 μl serum-free and anti-double-antibodies medium (Beijing Solarbio Science & Technology Co., Ltd.) and 5 μl 20 μmol siRNA stock solution were mixed. A total of 12 μl HiPerFect was added and left to stand for 15 min to form a transfection complex. The culture medium was discarded, then 1,863 μl anti-bibial antibody-free medium (Thermo Fisher Scientific, Inc.) and complex were added and cultured at 37˚C for 24 h). The protein level and mRNA levels were detected after 24 h. The following groups were used: Blank control, AngII + LBP, siNC, siNC + AngII + LBP, siRNA and siRNA + AngII + LBP.

RT-qPCR. A total RNA extraction kit (cat. no. DP171221; Tiangen Biotech Co., Ltd.) was used for RTAEC total RNA extraction. PrimeScript RT Master Mix (Perfect Real Time; cat. no. RR036B; Takara Bio, Inc.) was used for cDNA preparation. The reaction conditions were as follows: 37˚C for 15 min, 85˚C for 5 sec, 4˚C. Amplification was performed using TB Green Premix Ex Taq II (Tli RNase H Plus; cat. no. RR820B; Takara Bio, Inc.). The thermocycling conditions were as follows: 95˚C for 30 sec, 95˚C for 5 sec, 60˚C for 34 sec for 40 cycles. The primer sequences are listed in Table I. The $2^{-\Delta\Delta Cq}$ method (28) was used to calculate the mRNA expression levels of the target gene. β-actin was used as the reference gene.

Statistical analysis. SPSS22.0 (IBM Corp.) and GraphPad Prism6 software (GraphPad Software, Inc.) were used to analyze the data. Each experiment was repeated six times independently. Data are expressed as the mean ± SD. Data were analyzed using paired Student's t test or one-way ANOVA followed by Tukey's post hoc test. P<0.05 was considered to indicate a statistically significant difference.

Results

LBP attenuates serum oxidative stress in exhausted rats. ELISA was performed to study the antioxidant stress effect of LBP. Compared with the Control, there was no significant change in expression levels of AngII and T-AOC, while those of CAT increased and those of MDA and GSH decreased in the AE group. Compared with the AE group, expression levels of AngII and MDA in the EX group increased, whereas those of CAT, T-AOC and GSH expression levels decreased. These changes in MDA, T-AOC and GSH were significant. Compared with the EX group, the expression levels of AngII and MDA decreased in the EX + LBP group, whereas those of CAT, T-AOC and GSH increased (Fig. 1).

LBP attenuates thoracic aorta vascular and myocardial injury in exhausted rats. H&E staining was performed to study the protective effect of LBP on the thoracic aorta and myocardium of exhausted rats. H&E staining showed that the wall of the thoracic aorta of the Control group was intact and elastic fibers and endothelial cells were aligned. In the AE group, the interstitial wall of the thoracic aorta was slightly widened and the structure remained unchanged. Vascular endothelial cells in the thoracic aorta of the EX group were markedly lost, and the elastic fibers were broken, irregular and exhibited disordered arrangement. Compared with Ex group, the thoracic aorta endothelial cells in the EX + LBP group

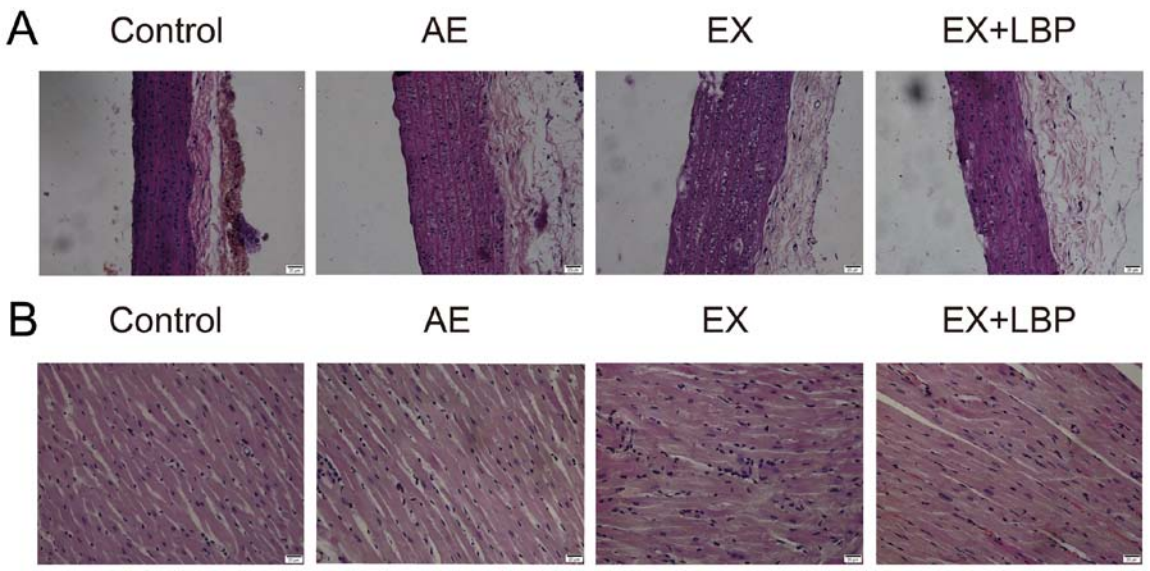

Figure 2. Effects of LBP and EX on the morphology and structure of thoracic aorta vessels and myocardium in rats. Morphological changes of (A) thoracic aorta and (B) myocardial tissue in rats were assessed by hematoxylin-eosin staining (magnification, x400). LBP, *Lycium barbarum* polysaccharide; EX, exhaustive exercise; AE, aerobic exercise.

were more complete, the elastic fibers arranged more regularly and exhibited less injury (Fig. 2A). Myocardial H&E staining showed that in the Control group, the myocardial fibers were slender, arranged neatly and connected to each other in a network, with a small amount of connective tissue between the myocardial fibers. The nucleus was oval and located in the center of the cell. Myocardial fibers of the AE group were arranged neatly and connected in a reticular pattern, and there was a small degree of inflammatory cell infiltration between myocardial fibers. The myocardial fibers of the EX group were disordered, turbid and unclear, the horizontal stripes disappeared and a large number of inflammatory cells infiltrated. The nuclei of myocardial cells in the EX + LBP group were slightly concentrated, myocardial fibers were swollen and there were few inflammatory cells (Fig. 2B).

LBP attenuates thoracic aorta vascular and myocardial apoptosis in exhausted rats. The anti-apoptotic effect of LBP on the thoracic aorta of exhausted rats was investigated by TUNEL staining. Compared with the Control, the positive expression of the thoracic aorta in the AE group increased slightly. Compared with the AE group, EX notably increased the positive expression of thoracic aorta blood vessels. Compared with the EX group, the positive expression of thoracic aorta blood vessels in the EX + LBP group was notably decreased (Fig. 3A). Compared with the Control, expression levels of Bax and caspase-3 in the myocardial tissue of the AE group decreased and those of Bcl-2 increased. Compared with the AE group, the expression levels of Bax and caspase-3 in myocardial tissue of the EX group increased, whereas those of Bcl-2 decreased. Compared with the EX group, the expression of Bax and caspase-3 in the myocardial tissue of the EX + LBP group decreased, whereas expression of Bcl-2 increased (Fig. 3B-D).

LBP attenuates thoracic aorta vascular and myocardial inflammation in exhausted rats by enhancing the Keap1/Nrf2 antioxidant stress pathway. Western blotting was performed to investigate whether LBP enhances the Keap1/Nrf2 antioxidant stress pathway in the thoracic aorta and myocardium of exhausted rats. Compared with the Control, the expression levels of TNF-α and Keap1 in thoracic aorta vascular tissue decreased and those of Nrf2, p-Nrf2 and GCLM increased. Compared with the AE group, expression of TNF-α in the EX group increased, and that of Keap1, Nrf2, GCLC, NQO1 and GCLM decreased. Compared with the EX group, expression of TNF-α and Keap1 in the EX + LBP group decreased, whereas that of Nrf2, p-Nrf2, GCLC, NQO1 and GCLM increased. (Fig. 4A). The rat myocardium western blotting results showed that, compared with the Control, the expression levels of TNF-α, p-Nrf2, GCLC, NQO1 and GCLM in the AE group increased. Compared with the AE group, the expression levels of TNF-α, GCLC and GCLM increased, whereas those of Nrf2, p-Nrf2 and NQO1 decreased in the EX group. Compared with the EX group, the expression levels of TNF-α and Keap1 in the EX + LBP group decreased and those of Nrf2, p-Nrf2, GCLM, GCLC and NQO1 increased (Fig. 4B).

The thoracic aorta vascular IHC results showed that, compared with the Control, positive expression of TNF-α and Keap1 in the nucleus decreased, whereas that of Nrf2 and GCLM increased in the AE group. Compared with the AE group, TNF-α positive expression in the EX group notably increased, while that of Nrf2, GCLC, NQO1 and GCLM decreased. Compared with the EX group, the positive expression of TNF-α in the nucleus decreased, and that of Nrf2, GCLC, NQO1 and GCLM increased in the EX + LBP group (Fig. 5A).

Rat myocardial IHC showed that, compared with the Control group, positive expression of GCLC and NQO1 in the AE group was increased, however no other notable changes were observed. Compared with the AE group, the positive expression of TNF-α in the nucleus of the EX group notably increased, while that of Keap1, GCLC

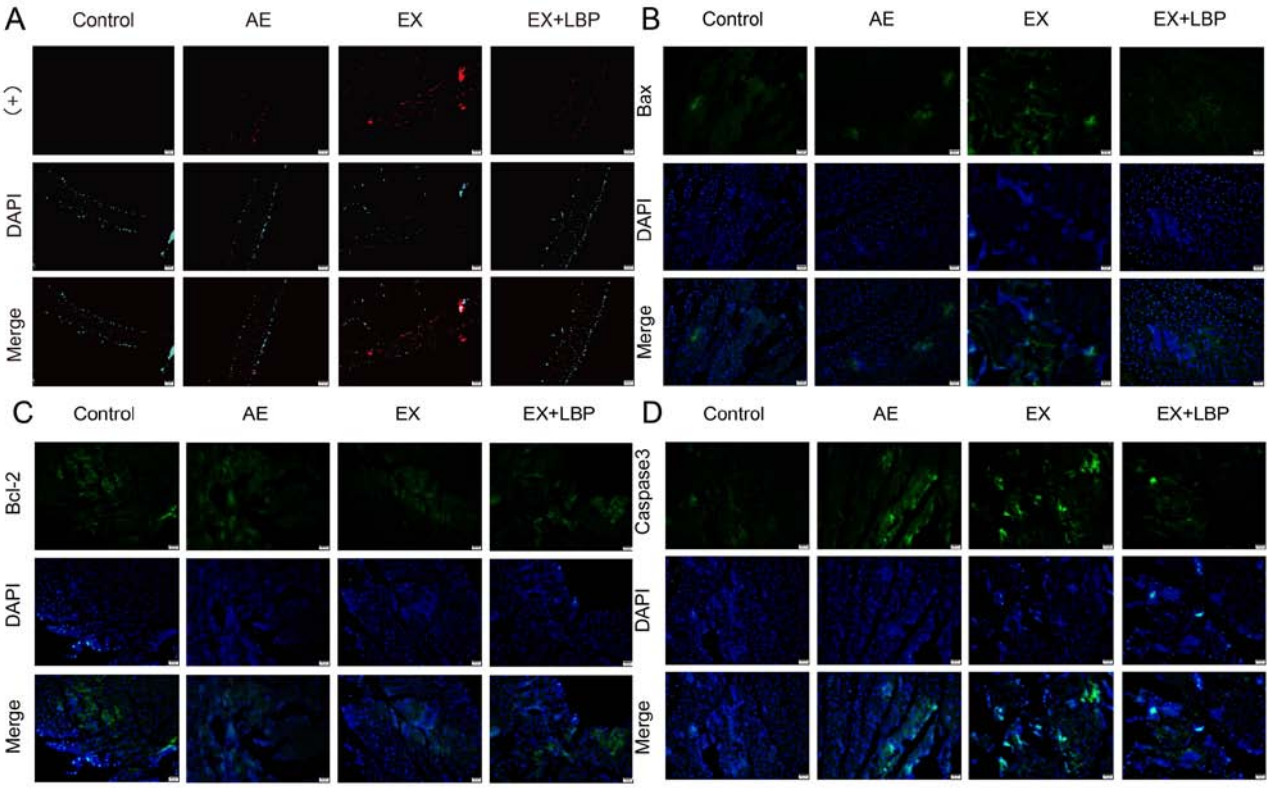

Figure 3. Effects of LBP and EX on thoracic aorta blood vessels and myocardial apoptosis in rats. (A) TUNEL staining was performed to detect apoptosis of rat thoracic aorta vascular cells. Immunofluorescence was performed to detect levels of (B) Bax, (C) Bcl-2 and (D) Caspase-3 in rat myocardial cells. Magnification, x400. LBP, *Lycium barbarum* polysaccharide; EX, exhaustive exercise; AE, aerobic exercise.

and NQO1 decreased. Compared with the EX group, the positive expression of TNF-α in the nucleus decreased, and that of Nrf2, NQO1 and GCLM increased in the EX + LBP group. (Fig. 5B).

LBP attenuates oxidative stress in RTAEC caused by AngII. In order to study the antioxidant effect of LBP, ELISA was performed. Compared with the Control, expression levels of CAT and GSH in the LBP group increased, and those of T-AOC exhibited no significant change. Compared with the LBP group, the expression levels of CAT, T-AOC and GSH in the AngII group decreased, and those of MDA, T-AOC and GSH increased. Compared with the AngII group, CAT expression in the AngII + LBP group increased, and that of MDA decreased (Fig. 6).

LBP attenuates expression of oxidative stress RTAEC inflammatory factors by enhancing the Keap1/Nrf2 antioxidant stress pathway. Western blotting was performed to investigate whether LBP enhances expression of the Keap1/Nrf2 antioxidant stress pathway in RTAEC. Compared with the Control, expression levels of TNF-α, p-Nrf2, NQO1 and GCLM in the LBP group increased, whereas those of Keap1 decreased. Compared with the LBP group, the expression of TNF-α increased and that of GCLC and GCLM decreased in the AngII group. Compared with the AngII group, the expression levels of TNF-α and Keap1 in the AngII + LBP group decreased, and those of Nrf2, NQO1, p-Nrf2, GCLC and GCLM increased. (Fig. 7).

Compared with the Control, the positive expression of activated Nrf2 in the nucleus of RTAECs in the LBP group increased, while GCLM in the cytoplasm did not notably change. Compared with the LBP group, the Nrf2 positive expression in the nucleus of the AngII group decreased and GCLM positive expression in the cytoplasm increased. Compared with the AngII group, the positive expression of Nrf2 in the cytoplasm and nucleus and GCLM in the cytoplasm increased in the AngII + LBP group (Fig. 8A and B).

RT-qPCR showed that, compared with the Control group, mRNA expression levels of Keap1 in the LBP group decreased; levels of TNF-α, IL-1β, Nrf2 and GCLC did not significantly change. Compared with the LBP group, mRNA expression levels of TNF-α and IL-1β in the AngII group increased and those of Keap1 and Nrf2 decreased. Compared with the AngII group, mRNA expression levels of TNF-α, IL-6, IL-1β and Keap1 in the AngII + LBP group decreased, whereas those of Nrf2, NQO1, GCLC and GCLM increased (Fig. 9).

Transfection of RTAEC with siNrf2 attenuates protein expression of Nrf2 and p-Nrf2. In order to study whether LBP reduction of oxidative stress-induced cardiovascular damage is related to the enhancement of keap1/Nrf2 anti-oxidative stress signaling pathway in endothelial cells, *in vitro* experiments were performed for siRNA transfection. Transfection efficiency was determined by transfection of RTAECs with fluorescence-labeled blank siRNA (Fig. 10A). Cell transfection efficiency was highest at a transfection concentration of 50 nmol and 24 h after transfection. The optimal transfection concentration and time were determined (Fig. 10B). The

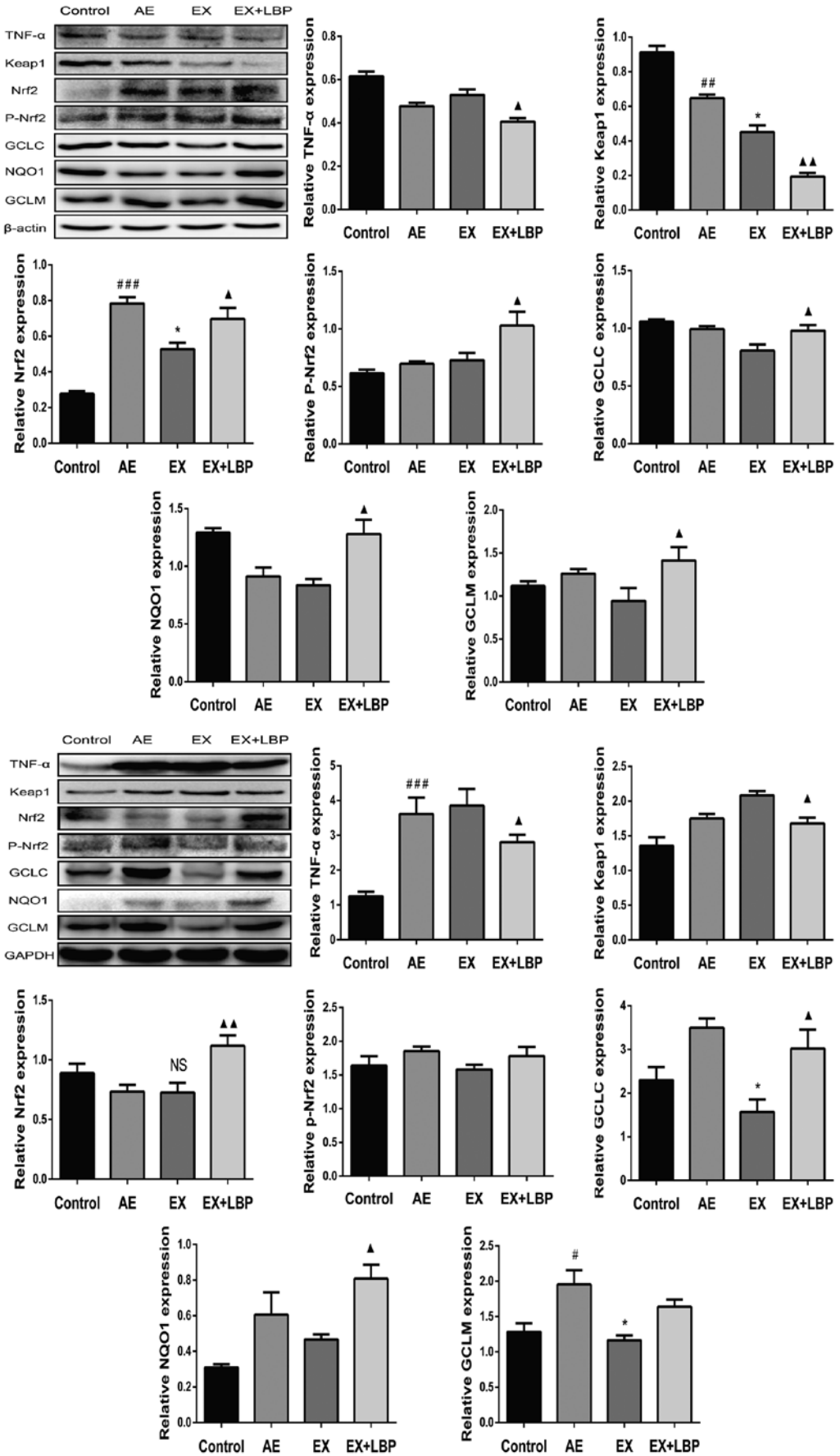

Figure 4. Effects of LBP and EX on protein expression levels of TNF-α, Keap1, Nrf2, p-Nrf2, GCLC, NQO1 and GCLM in thoracic aorta and myocardial tissue of rats. Western blot analysis of expression of TNF-α, Keap1, Nrf2, p-Nrf2, GCLC, NQO1 and GCLM protein in rat (A) thoracic aorta vascular and (B) myocardial tissue. $^{\#}$P<0.01, $^{\#\#\#}$P<0.001 vs. Control; NS, *P<0.05 vs. AE; $^{\blacktriangle}$P<0.05, $^{\blacktriangle\blacktriangle}$P<0.01 vs. EX. LBP, *Lycium barbarum* polysaccharide; EX, exhaustive exercise; Keap1, Kelch-like ECH-associated protein 1; p-, phosphorylated; Nrf2, NF-E2-related factor 2; NQO1, quinone oxidoreductase 1; GCLC, glutamyl-cysteine synthetase catalytic subunit; GCLM, glutamate-cysteine ligase modified subunit; NS, no significance; AE, aerobic exercise.

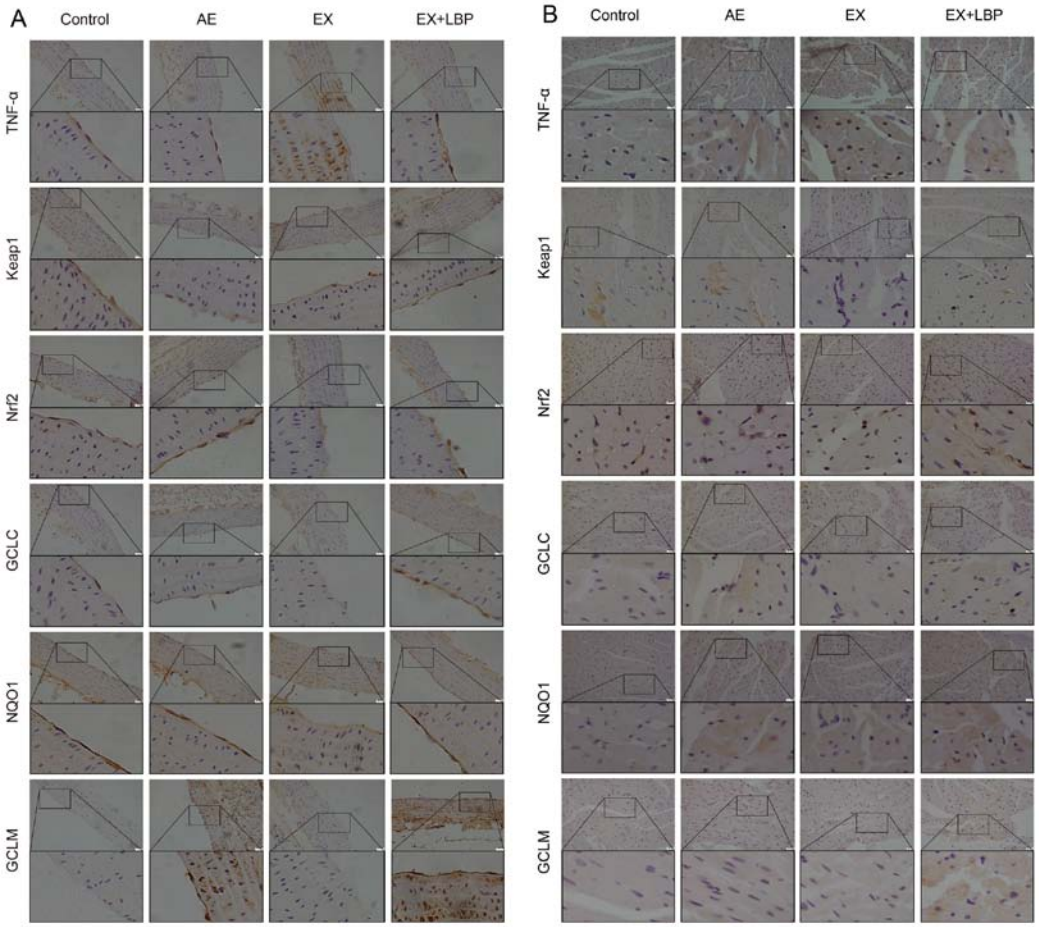

Figure 5. Effect of LBP and EX on protein expression levels of TNF-α, Keap1, Nrf2, GCLC, NQO1 and GCLM in rat thoracic aorta and myocardial tissue. Immunohistochemistry was performed to detect the protein expression levels of TNF-α, Keap1, Nrf2, GCLC, NQO1 and GCLM in rat (A) thoracic aorta vascular and (B) myocardial tissue. Magnification, x400. LBP, *Lycium barbarum* polysaccharide; EX, exhaustive exercise; Keap1, Kelch-like ECH-associated protein 1; Nrf2, NF-E2-related factor 2; NQO1, quinone oxidoreductase 1; GCLC, glutamyl-cysteine synthetase catalytic subunit; GCLM, glutamate-cysteine ligase modified subunit; AE, aerobic exercise.

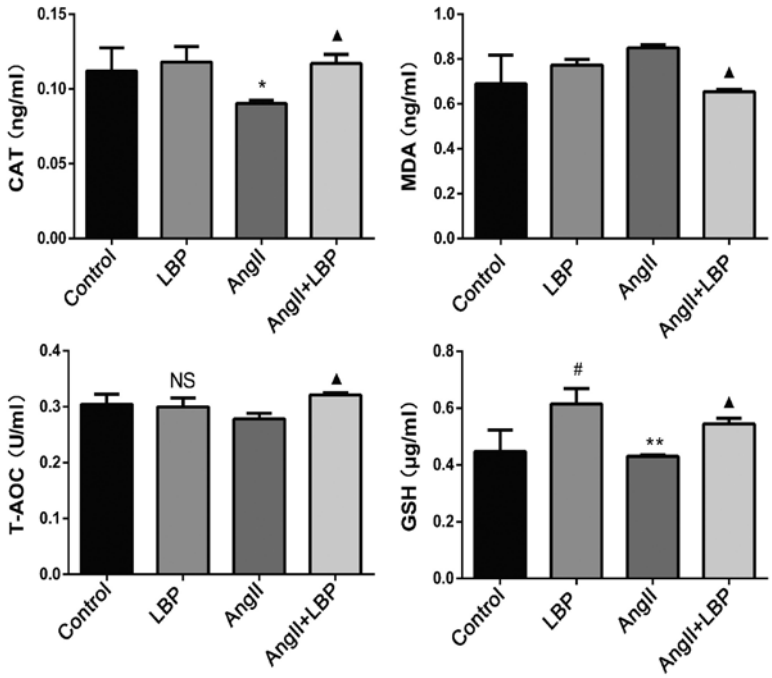

Figure 6. Effect of LBP and AngII on expression levels of CAT, MDA, T-AOC and GSH in rat thoracic aortic endothelial cell supernatant. NS, $^{\#}$P<0.05 vs. Control; *P<0.05, **P<0.01 vs. LBP; $^{\blacktriangle}$P<0.05 vs. AngII. LBP, *Lycium barbarum* polysaccharide; AngII, angiotensin II; CAT, catalase; MDA, malonaldehyde; T-AOC, total antioxidation capacity; GSH, glutathione; NS, no significance.

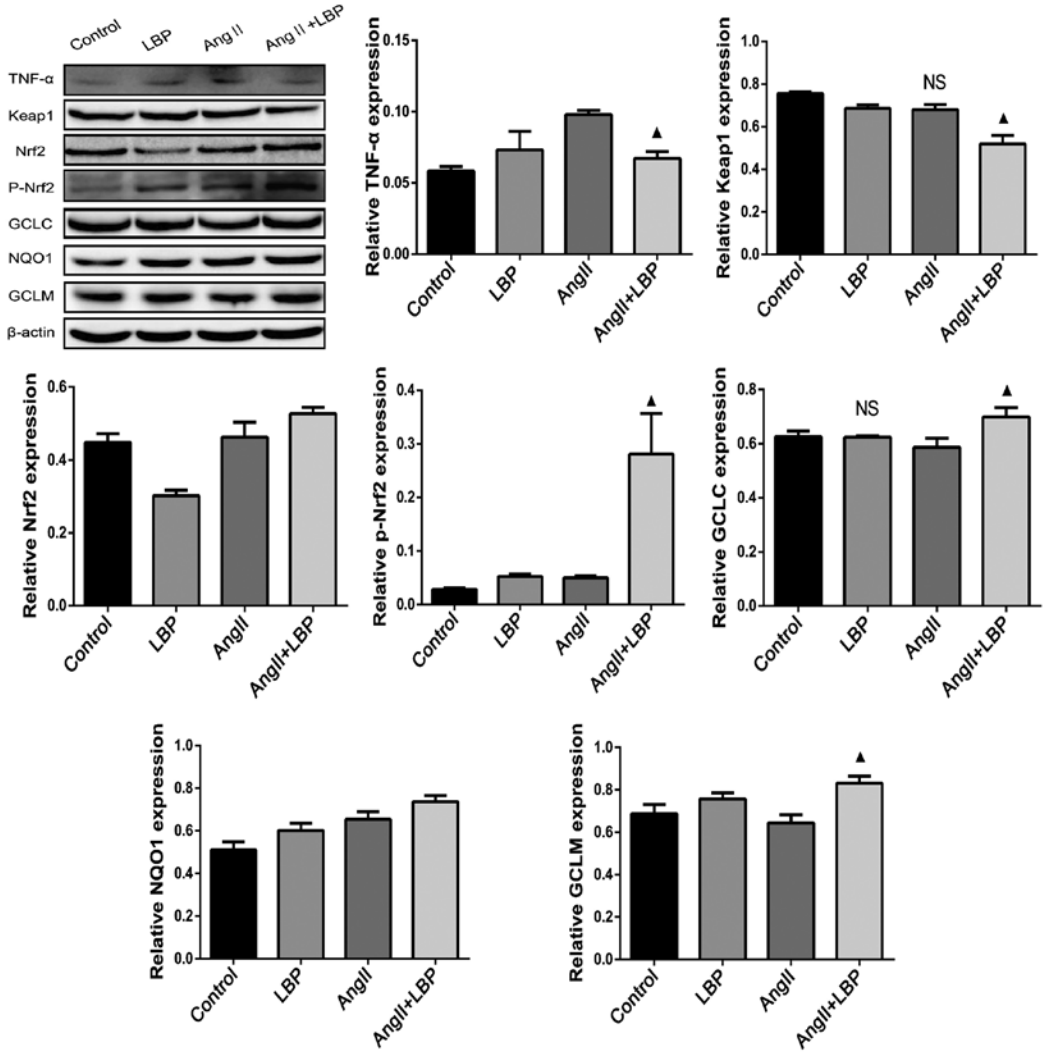

Figure 7. Effects of LBP and AngII on expression levels of TNF-α, Keap1, Nrf2, p-Nrf2, GCLC, NQO1 and GCLM in rat thoracic aortic endothelial cells. NS vs. Control and LBP; ▲P<0.05 vs. AngII. LBP, *Lycium barbarum* polysaccharide; AngII, angiotensin II; Keap1, Kelch-like ECH-associated protein 1; p-, phosphorylated; Nrf2, NF-E2-related factor 2; NQO1, quinone oxidoreductase 1; GCLC, glutamyl-cysteine synthetase catalytic subunit; GCLM, glutamate-cysteine ligase modified subunit; NS, no significance.

silencing efficiency of siRNA3, siRNA4 and siRNA5 was detected based on the transfection concentration and time; siRNA5 exhibited the best silencing effect and was selected for subsequent experiments. Expression levels of Nrf2 and p-Nrf2 protein in the siRNA5 group were significantly lower than in the Control (P<0.05 and P<0.01). Western blotting showed that, compared with the AngII + LBP group, protein expression levels of Nrf2 and p-Nrf2 in the siRNA + AngII + LBP group decreased (Fig. 10C).

siNrf2 attenuates antioxidant stress of LBP. ELISA was performed to study the antioxidant effect of LBP on siNrf2. Compared with the Control, the expression levels of CAT, T-AOC and GSH in the AngII group decreased and those of MDA increased. Compared with the AngII group, the expression levels of CAT, T-AOC and GSH in the AngII + LBP group increased, while those of MDA decreased. Compared with the AngII + LBP group, the expression levels of CAT, T-AOC and GSH in the siRNA + AngII + LBP group decreased, and those of MDA increased. Compared with siNC + AngII + LBP group, the MDA expression levels increased, and those of GSH and T-AOC decreased in the siRNA + AngII + LBP group (Fig. 11).

siNrf2 attenuates anti-inflammatory effects of LBP. In order to study the effect of siNrf2 on the anti-inflammatory effect of LBP, RT-qPCR was performed. Compared with the Control, the expression levels of TNF-α, IL-6 and IL-1β increased in the AngII group. Compared with the AngII group, the expression levels of TNF-α, IL-6 and IL-1β decreased. Compared with the AngII + LBP group, expression levels of TNF-α, IL-6 and IL-1β in the siRNA + AngII + LBP group increased. Compared with the siNC + AngII + LBP group, expression of TNF-α was increased in the siRNA + AngII + LBP group. Compared with the siRNA group, expression levels of TNF-α, IL-1β and IL-6 in the siRNA + AngII + LBP group increased (Fig. 12).

Flow cytometry showed that, compared with the Control, the expression of TNF-α in the AngII group increased. Compared with the siNC group, expression of TNF-α in the siNC + AngII + LBP group decreased. Compared with the AngII + LBP group, expression of TNF-α increased in the siRNA + AngII + LBP group (Fig. 13).

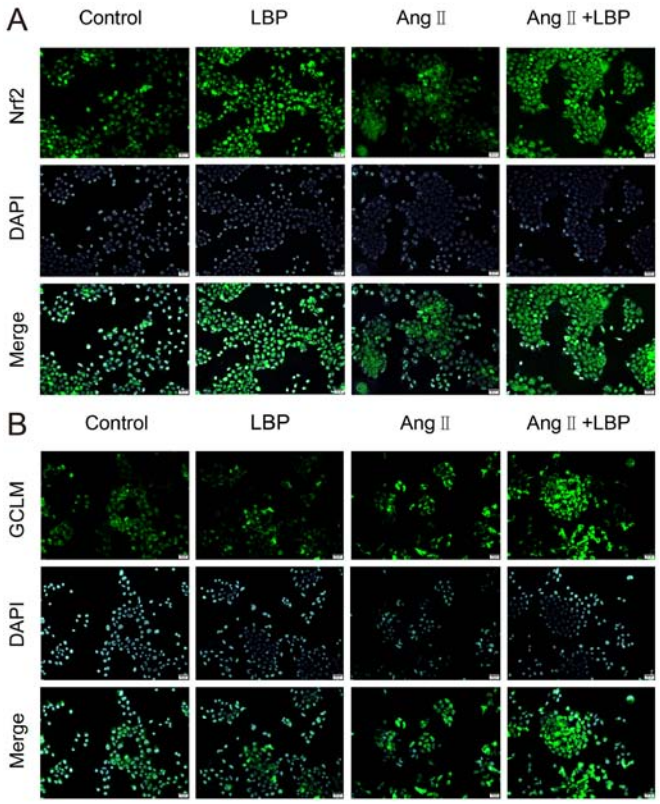

Figure 8. Effect of LBP and AngII on Nrf2 and GCLM protein expression in rat thoracic aortic endothelial cells. Immunofluorescence was used to detect protein expression levels of (A) Nrf2 and (B) GCLM. Magnification, x400. LBP, *Lycium barbarum* polysaccharide; AngII, angiotensin II; Nrf2, NF-E2-related factor 2; GCLM, glutamate-cysteine ligase modified subunit.

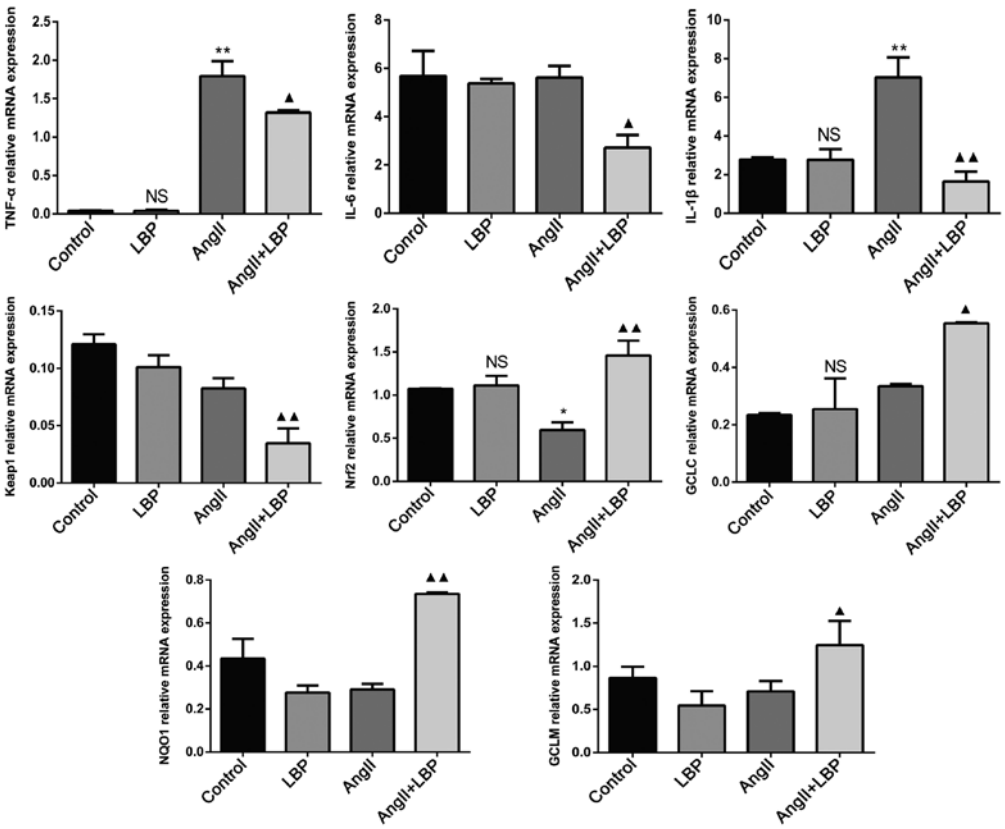

Figure 9. Effects of LBP and AngII on mRNA expression of TNF-α, IL-6, IL-1β, Keap1, Nrf2, GCLC, NQO1 and GCLM in rat thoracic aortic endothelial cells. NS, *P<0.05 vs. Control; **P<0.01 vs. LBP; $^{▲}$P<0.05, $^{▲▲}$P<0.01 vs. AngII. LBP, *Lycium barbarum* polysaccharide; AngII, angiotensin II; Keap1, Kelch-like ECH-associated protein 1; Nrf2, NF-E2-related factor 2; NQO1, quinone oxidoreductase 1; GCLC, glutamyl-cysteine synthetase catalytic subunit; GCLM, glutamate-cysteine ligase modified subunit; NS, no significance.

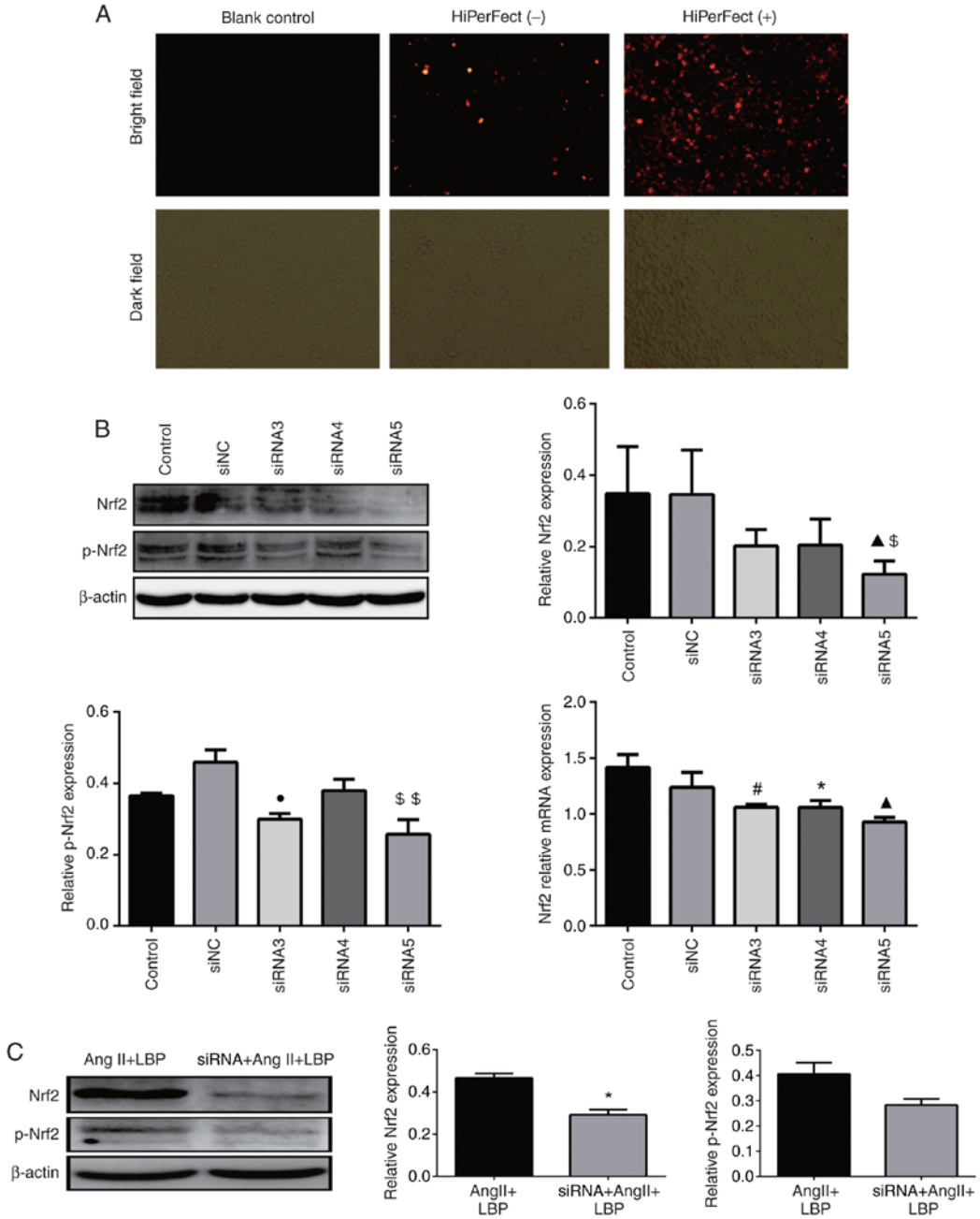

Figure 10. Effect of siNrf2 on protein expression levels of Nrf2 and p-Nrf2 in RTAEC. (A) RTAEC imaged under a fluorescence microscope 24 h after transfection (magnification, x400). (B) Screening for the best siRNA by western blot analysis and reverse transcription-quantitative PCR. $^{\#}$P<0.05, *P<0.05, $^{\blacktriangle}$P<0.05 vs. Control; $^{\bullet}$P<0.05 vs. siNC; $^{\$}$P<0.05, $^{\$\$}$P<0.01 vs. siNC. (C) Expression levels of Nrf2 and p-Nrf2 protein in RTAEC. *P<0.05 vs. AngII + LBP. si, small interfering; Nrf2, NF-E2-related factor 2; p-, phosphorylated; RTAEC, rat thoracic aortic endothelial cell; NC, non-specific control.

Discussion

Moderate AE decreases oxidative stress and inflammation, but excessive exercise increases the level of oxidative stress in the body (29). Studies have shown that long-term oxidative stress induces a high-load state in the heart and blood vessels and causes cardiovascular disease, including atherosclerosis, heart failure and myocardial fibrosis (30-32). Therefore, decreasing oxidative stress and inflammation is key to preventing cardiovascular system injury.

As a key transcription factor of the Keap1/Nrf2 signaling pathway, Nrf2 serves an important role in maintaining the balance of oxidative stress in the body (10,11). Nrf2 and its downstream transcriptional proteins GCLC, GCLM and NQO1 slow the development of disease, including bronchial asthma and chronic obstructive pulmonary disease, by inhibiting oxidative stress in the lungs (33). They also decrease liver injury due to oxidative stress caused by the excessive use of acetaminophen (34). In recent years, LBP has been widely studied due to its anti-inflammatory and antioxidant effects, which not only protect the heart (35), but also decrease oxidative stress in the retina of diabetic rats and serve a neuroprotective role (36). LBP pretreatment decreases toxic damage in the liver caused by cadmium-induced oxidative stress (37). Based on the aforementioned findings, it was hypothesized that LBP may decrease oxidative stress and cardiovascular system

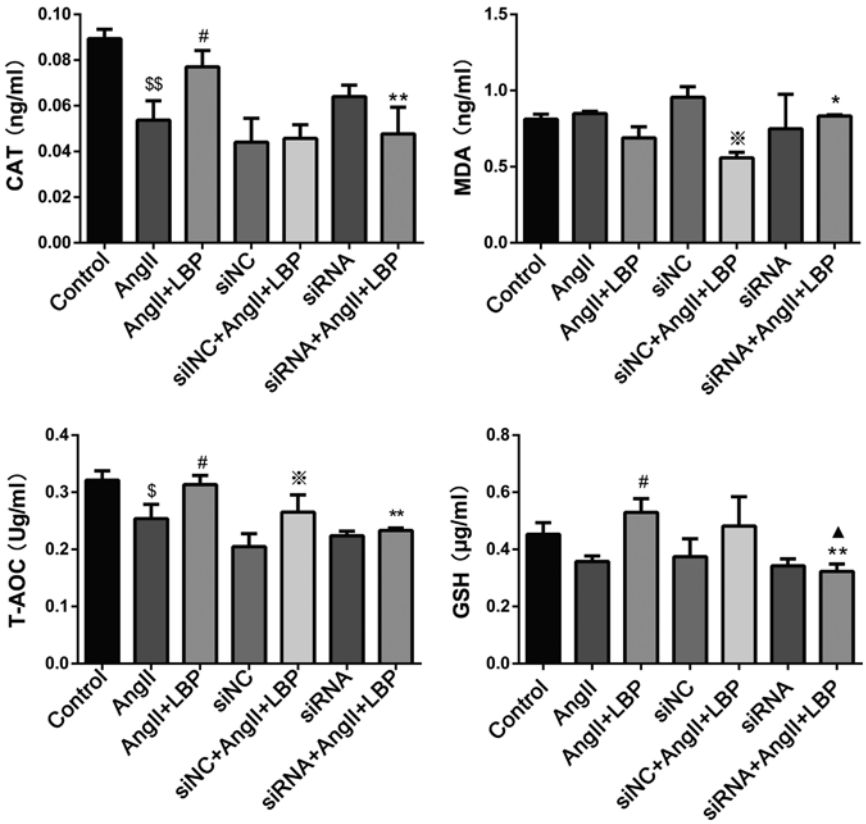

Figure 11. Effect of siNrf2 on expression levels of CAT, MDA, T-AOC and GSH in rat thoracic aortic endothelial cell supernatant. $^{\$}$P<0.05; $^{\$\$}$P<0.01 vs. Control; $^{\#}$P<0.05 vs. AngII; *P<0.05, **P<0.01 vs. AngII + LBP; $^{※}$P<0.05 vs. siNC; $^{▲}$P<0.05 vs. siNC + AngII + LBP. si, small interfering; Nrf2, NF-E2-related factor 2; CAT, catalase; MDA, malonaldehyde; T-AOC, total antioxidation capacity; GSH, glutathione; AngII, angiotensin II; LBP, *Lycium barbarum* polysaccharide; NC, non-specific control.

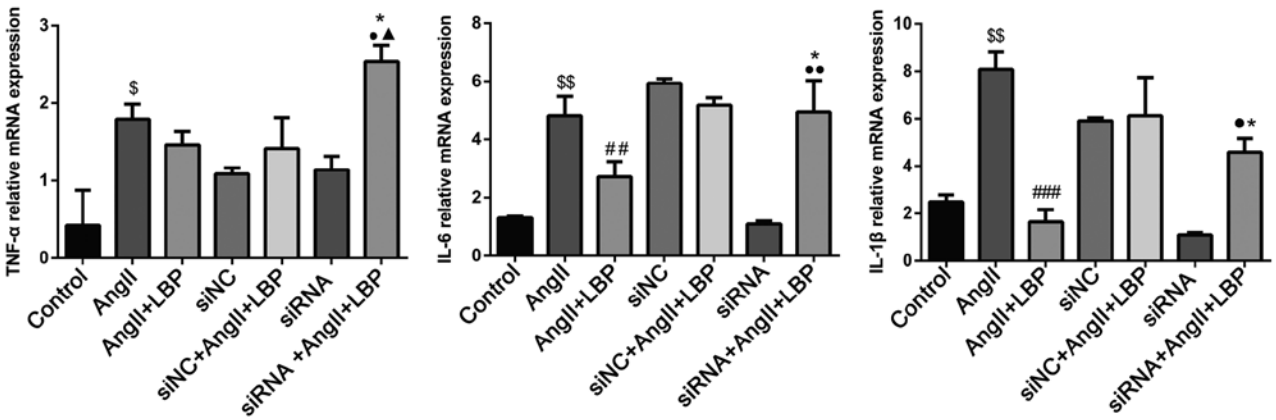

Figure 12. Effect of siNrf2 on mRNA expression levels of TNF-α, IL-6, IL-1β in rat thoracic aortic endothelial cells. $^{\$}$P<0.05, $^{\$\$}$P<0.01 vs. Control; $^{\#\#}$P<0.01, $^{\#\#\#}$P<0.001 vs. AngII; P<0.05 vs. AngII + LBP; $^{※}$P<0.05 vs. siNC; $^{▲}$P<0.05 vs. siNC + AngII + LBP; $^{●}$P<0.05, $^{●●}$P<0.01 vs. siRNA. si, small interfering; Nrf2, NF-E2-related factor 2; AngII, angiotensin II; LBP, *Lycium barbarum* polysaccharide; NC, non-specific control.

injury caused by EX via enhanced Keap1/Nrf2 signaling pathway.

Under stress, the body activates the renin-Ang system, which increases the content of AngII and aggravates oxidative stress and inflammation in the body (38). SOD and CAT regulate oxidative stress and free radicals, MDA reflects the degree of oxidative stress and T-AOC reflects the total antioxidant level of all antioxidant stress indexes (39-41). Aerobic intermittent training decreases expression levels of MDA and inflammatory factors in serum and increases those of CAT and GSH (42). The concentration of GSH peroxidase, GLU and MDA in the serum of athletes increases along with expression levels of TNF-α, whereas those of CAT decrease following anti-gravity exercise (43). The *in vivo* experiment showed that expression levels of AngII and MDA in the serum increased, those of CAT, T-AOC and GSH decreased and expression of TNF-α protein in the blood vessels and myocardium increased in the EX group. Compared with the EX group, the level of MDA in the serum decreased, the levels of CAT, T-AOC and GSH increased and expression of TNF-α protein in blood

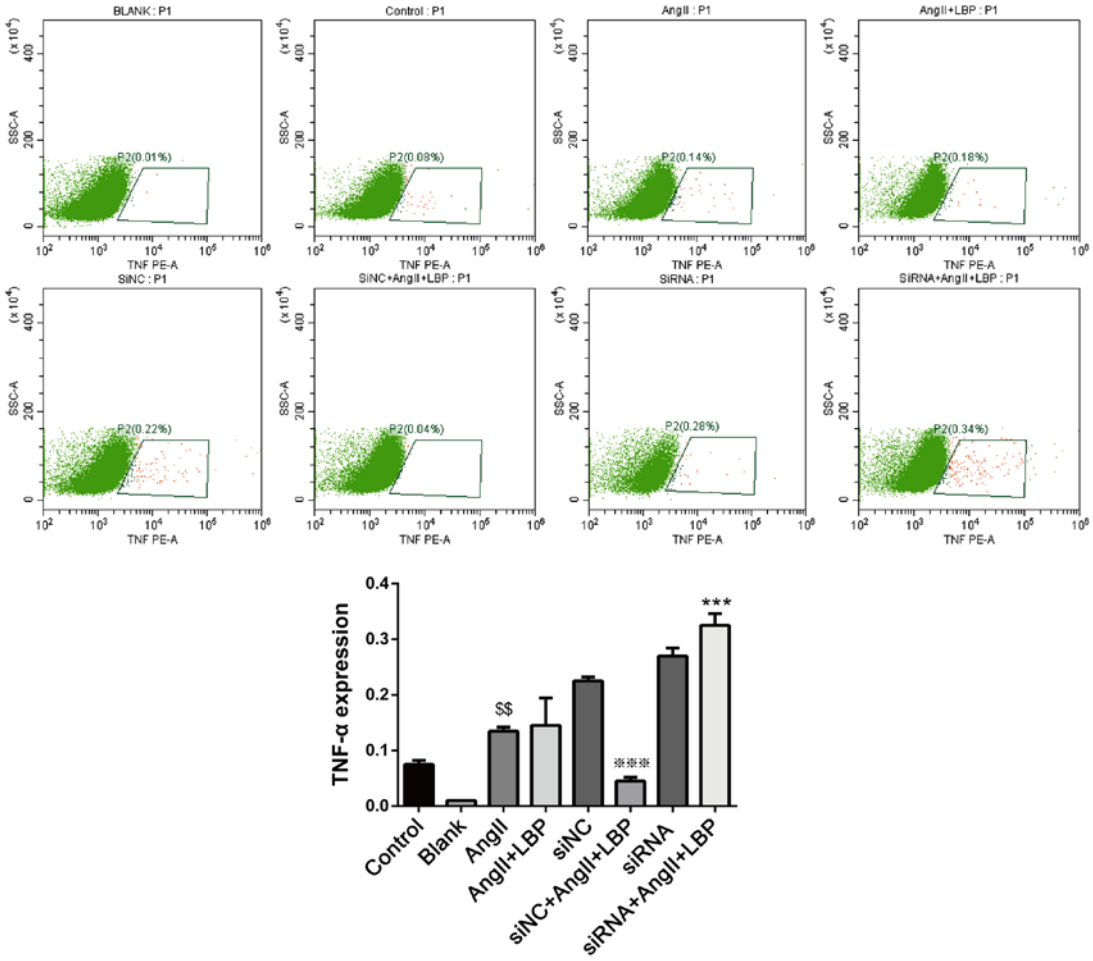

Figure 13. Effect of siNrf2 on expression of TNF-α in rat thoracic aortic endothelial cells. $^{\$\$}$P<0.01 vs. Control; ***P<0.001 vs. AngII + LBP; $^{\#\#\#}$P<0.001 vs. siNC. si, small interfering; Nrf2, NF-E2-related factor 2; AngII, angiotensin II; LBP, *Lycium barbarum* polysaccharide; NC, non-specific control.

vessels and myocardium decreased in the EX + LBP group, suggesting that LBP relieved oxidative stress and inflammation and exhibited an anti-oxidative stress and anti-inflammatory effect.

Apoptosis is a type of programmed cell death. There are two main pathways of apoptosis: Death receptor-mediated apoptosis and mitochondrial/cytochrome C-mediated apoptosis. The former is primarily associated with caspase-8 and the latter with caspase-9. Activated caspase-9 activates caspase-3 to cause apoptosis, and anti-apoptotic proteins, such as Bcl-2, serve an anti-apoptotic role (44). The pro-apoptotic protein Bax promotes apoptosis in cells (45-47). Aerobic endurance exercise results in downregulation of Bax and caspase-3 and upregulation of Bcl-2 (48,49). EX causes severe myocardial ischemia and hypoxia, increases cardiomyocyte apoptosis, significantly increases expression of Bax and caspase-3 protein and significantly decreases protein expression of Bcl-2 (50,51). The *in vivo* experiment showed that the expression of Bax and caspase-3 decreased and that of Bcl-2 increased in the myocardium of rats in the EX group, and the thoracic aorta exhibited different degrees of injury and cell apoptosis, which was consistent with the aforementioned results. Compared with the EX group, vascular and myocardial apoptosis of the thoracic aorta in the EX + LBP group decreased, indicating that LBP serves an anti-apoptotic effect and protects the cardiovascular system.

Enhancing the Keap1/Nrf2 pathway improves the antioxidant stress response and serve a protective role in the body (52). The results of the *in vivo* experiment showed that excessive oxidative stress decreased expression of Nrf2, GCLC, NQO1 and GCLM in the blood vessels and myocardium. Compared with the EX group, expression levels of Keap1 in the blood vessels and myocardium decreased and those of Nrf2, p-Nrf2, GCLC, NQO1 and GCLM increased in the EX + LBP group. It has been suggested that LBP enhances the expression of the Keap1/Nrf2 pathway in the myocardium and blood vessels and serves an antioxidant role.

LBP enhances expression of the Keap1/Nrf2 antioxidant signaling pathway in the myocardium and blood vessels to further recover the tissue damage and apoptosis caused by excessive oxidative stress and inflammation caused by EX, and it serves a role in protecting the cardiovascular system, which was consistent with the initial hypothesis.

As the first line of defense of the cardiovascular system, endothelial cells serve a key role in maintaining smooth vascular wall, normal blood flow and normal cardiovascular system metabolism. Oxidative stress-induced endothelial cell injury is an important mechanism of cardiovascular disease (53). Endothelial cells serve a key role in protecting the cardiovascular system; LBP enhances the expression of antioxidant stress proteins in endothelial cells in

myocardial and vascular tissue. Therefore, it was hypothesized that excessive oxidative stress leads to loss of cardiovascular endothelial cells and cardiovascular system protection, which promotes cardiovascular system injury. LBP enhances endothelial antioxidant capacity by enhancing expression of the Keap1/Nrf2 antioxidant signaling pathway in endothelial cells recovering the cardiovascular system.

In the *in vitro* experiment, AngII was used to prepare an RTAEC oxidative stress model. Expression of MDA in the supernatant of endothelial cells treated with AngII increased, while that of CAT, T-AOC and GSH decreased. At the same time, protein expression of TNF-α increased and mRNA expression of IL-1 β, IL-6 and TNF-α increased; this was reversed following LBP intervention. Compared with the AngII group, Nrf2, GCLC, NQO1 and GCLM protein and mRNA expression increased in the AngII + LBP group; Nrf2 and GCLM expression decreased in the AngII group but was increased following LBP intervention. LBP enhances the Keap1/Nrf2 antioxidant stress signaling pathway to decrease oxidative stress and inflammation in endothelial cells. In order to verify whether LBP decreases the oxidative stress state of endothelial cells and whether inflammation serves a role in the Keap1/Nrf2 antioxidant stress signaling pathway, Nrf2-specific siRNA transfection was performed. The expression levels of total and p-Nrf2 protein decreased following siNrf2 transfection into endothelial cells. At the same time, the anti-inflammatory and oxidative stress effects of LBP were weakened by siNrf2. LBP counteracted the increase in oxidative stress and inflammatory factors in endothelial cells induced by AngII via enhancement of the Keap1/Nrf2 signaling pathway.

In conclusion, by decreasing the oxidative stress state and inflammatory response of endothelial cells, LBP enhances expression of the Keap1/Nrf2 antioxidant signaling pathway and alleviates the oxidative stress state in the body and myocardial vascular tissue injury, thus protecting the cardiovascular system.

Acknowledgements

Not applicable.

Funding

This study was supported by the National Natural Science Foundation of China (grant nos. 81560052 and 81760055) and Ningxia Natural Science Foundation (grant nos. 2020AAC03364 and 2020AAC03141).

Availability of data and materials

All data generated or analyzed during this study are included in this published article.

Authors' contributions

GL, LW and LZ conceptualized and designed the experiment. GL and LW reviewed the manuscript. XH performed the experiments, analyzed the data and wrote the manuscript. LM performed the experiments. XC and LN performed the data analysis. XH and LM confirm the authenticity of all the raw data. All authors read and approved the final manuscript.

Ethics approval and consent to participate

The present study was approved by the Ethics Committee for Animal Experiments.

Patient consent for publication

Not applicable.

Competing interests

The authors declare that they have no competing interests.

References

1. Schmied C, Loidl M, Rossi V, La Puente de Battre MD, Reich B, Josef N and Niederseer D: Dose-response relationship of active commuting to work: Results of the GISMO study. Scand J Med Sci Sports 30 (Suppl 1): 50-58, 2020.
2. Fitze DP, Franchi M, Popp WL, Ruoss S, Catuogno S, Camenisch K, Lehmann D, Schmied CM, Niederseer D, Frey WO, *et al*: Concentric and eccentric pedaling-type interval exercise on a soft robot for stable coronary artery disease patients: Toward a personalized protocol. JMIR Res Protoc 8: e10970, 2019.
3. Di Meo S, Napolitano G and Venditti P: Mediators of physical activity protection against ROS-linked skeletal muscle damage. Int J Mol Sci 20: 3024, 2019.
4. Liu B, Liu W, Liu P, Liu X, Song X, Hayashi T, Onodera S and Ikejima T: Silibinin alleviates the learning and memory defects in overtrained rats accompanying reduced neuronal apoptosis and senescence. Neurochem Res 44: 1818-1829, 2019.
5. Moretti R and Caruso P: The controversial role of homocysteine in neurology: From labs to clinical practice. Int J Mol Sci 20: 231, 2019.
6. Koller A, Szenasi A, Dornyei G, Kovacs N, Lelbach A and Kovacs I: Coronary microvascular and cardiac dysfunction due to homocysteine pathometabolism; a complex therapeutic design. Curr Pharm Des 24: 2911-2920, 2018.
7. Li X, Hou J, Du J, Feng J, Yang Y, Shen Y, Chen S, Feng J, Yang D, Li D, *et al*: Potential protective mechanism in the cardiac microvascular injury. Hypertension 72: 116-127, 2018.
8. Stancu CS, Toma L and Sima AV: Dual role of lipoproteins in endothelial cell dysfunction in atherosclerosis. Cell Tissue Res 349: 433-446, 2012.
9. Karan A, Bhakkiyalakshmi E, Jayasuriya R, Sarada DV and Ramkumar KM: The pivotal role of nuclear factor erythroid 2-related factor 2 in diabetes-induced endothelial dysfunction. Pharmacol Res 153: 104601, 2020.
10. Li LH, Peng WN, Deng Y, Li JJ and Tian XR: Action of trichostatin A on Alzheimer's disease-like pathological changes in SH-SY5Y neuroblastoma cells. Neural Regen Res 15: 293-301, 2020.
11. Fão L, Mota SI and Rego AC: Shaping the Nrf2-ARE-related pathways in Alzheimer's and Parkinson's diseases. Ageing Res Rev 54: 100942, 2019.
12. Zheng D, Liu Z, Zhou Y, Hou N, Yan W, Qin Y, Ye Q, Cheng X, Xiao Q, Bao Y, *et al*: Urolithin B, a gut microbiota metabolite, protects against myocardial ischemia/reperfusion injury via p62/Keap1/Nrf2 signaling pathway. Pharmacol Res 153: 104655, 2020.
13. Li M, Huang W, Jie F, Wang M, Zhong Y, Chen Q and Lu B: Discovery of Keap1-Nrf2 small-molecule inhibitors from phytochemicals based on molecular docking. Food Chem Toxicol 133: 110758, 2019.
14. Zimta AA, Cenariu D, Irimie A, Magdo L, Nabavi SM, Atanasov AG and Berindan-Neagoe I: The role of Nrf2 activity in cancer development and progression. Cancers (Basel) 11: 1755, 2019.
15. Cui B, Zhang S, Wang Y and Guo Y: Farrerol attenuates β-amyloid-induced oxidative stress and inflammation through Nrf2/Keap1 pathway in a microglia cell line. Biomed Pharmacother 109: 112-119, 2019.

16. Wang Y, Han Q, Bai F, Luo Q, Wu M, Song G, Zhang H and Wang Y: The assembly and antitumor activity of *lycium barbarum* polysaccharide-platinum-based conjugates. J Inorg Biochem 205: 111001, 2020.
17. Lakshmanan Y, Wong FSY, Zuo B, So KF, Bui BV and Chan HH: Posttreatment intervention with *Lycium Barbarum* polysaccharides is neuroprotective in a rat model of chronic ocular hypertension. Invest Ophthalmol Vis Sci 60: 4606-4618, 2019.
18. Zhang L, Gao X, Qin Z, Shi X, Xu K, Wang S, Tang M, Wang W, Gao S, Zuo L, *et al*: USP15 participates in DBP-induced testicular oxidative stress injury through regulating the Keap1/Nrf2 signaling pathway. Sci Total Environ 783: 146898, 2021.
19. Lou L, Chen G, Zhong B and Liu F: *Lycium barbarum* polysaccharide induced apoptosis and inhibited proliferation in infantile hemangioma endothelial cells via down-regulation of pI3K/AKT signaling pathway. Biosci Rep: Aug 19,2019 (Epub ahead of print). doi: 10.1042/BSR20191182.
20. Ding Y, Yan Y, Chen D, Ran L, Mi J, Lu L, Jing B, Li X, Zeng X and Cao Y: Modulating effects of polysaccharides from the fruits of *Lycium barbarum* on the immune response and gut microbiota in cyclophosphamide-treated mice. Food Funct 10: 3671-3683, 2019.
21. Kwok SS, Bu Y, Lo AC, Chan TC, So KF, Lai JS and Shih KC: A systematic review of potential therapeutic use of *Lycium Barbarum* polysaccharides in disease. BioMed Res Int 2019: 4615745, 2019.
22. Wu Q, Liu LT, Wang XY, Lang ZF, Meng XH, Guo SF, Yan B, Zhan T, Zheng HZ and Wang HW: *Lycium barbarum* polysaccharides attenuate kidney injury in septic rats by regulating Keap1-Nrf2/ARE pathway. Life Sci 242: 117240, 2020.
23. Zhu W, Zhou S, Liu J, McLean RJC and Chu W: Prebiotic, immuno-stimulating and gut microbiota-modulating effects of *Lycium barbarum* polysaccharide. Biomed Pharmacother 121: 109591, 2020.
24. Ni H, Wang G, Xu Y, Gu X, Sun C and Li H: *Lycium barbarum* polysaccharide alleviates IL-1β-evoked chondrogenic ATDC5 cell inflammatory injury through mediation of microRNA-124. Artif Cells Nanomed Biotechnol 47: 4046-4052, 2019.
25. Song Q, Zhou ZJ, Cai S, Chen Y and Chen P: Oxidative stress links the tumour suppressor p53 with cell apoptosis induced by cigarette smoke. Int J Environ Health Res: Apr 7, 2021 (Epub ahead of print). doi: 10.1080/09603123.2021.1910211.
26. Jie YK, Cheng CH, Wang LC, Ma HL, Deng YQ, Liu GX, Feng J, Guo ZX and Ye LT: Hypoxia-induced oxidative stress and transcriptome changes in the mud crab (*Scylla paramamosain*). Comp Biochem Physiol C Toxicol Pharmacol 245: 109039, 2021.
27. Thomas DP and Marshall KI: Effects of repeated exhaustive exercise on myocardial subcellular membrane structures. Int J Sports Med 9: 257-260, 1988.
28. Livak KJ and Schmittgen TD: Analysis of relative gene expression data using real-time quantitative PCR and the 2(-ΔΔC(T)) method. Methods 25: 402-408, 2001.
29. Luca M and Luca A: Oxidative stress-related endothelial damage in vascular depression and vascular cognitive impairment: beneficial effects of aerobic physical exercise. Oxid Med Cell Longev 2019: 8067045, 2019.
30. Zhang X, Wang Y, Zhao R, Hu X, Zhang B, Lv X, Guo Z, Zhang Z, Yuan J, Chu X, *et al*: Folic acid supplementation suppresses sleep deprivation-induced telomere dysfunction and senescence-associated secretory phenotype (SASP). Oxid Med Cell Longev 2019: 4569614, 2019.
31. Kura B, Szeiffova Bacova B, Kalocayova B, Sykora M and Slezak J: Oxidative stress-responsive MicroRNAs in heart injury. Int J Mol Sci 21: 358, 2020.
32. Xiang W, Wang L, Cheng S, Zhou Y and Ma L: Protective effects of α-lipoic acid on vascular oxidative stress in rats with hyperuricemia. Curr Med Sci 39: 920-928, 2019.
33. Mizumura K, Maruoka S, Shimizu T and Gon Y: Role of Nrf2 in the pathogenesis of respiratory diseases. Respir Investig 58: 28-35, 2020.
34. Luo DD, Chen JF, Liu JJ, Xie JH, Zhang ZB, Gu JY, Zhuo JY, Huang S, Su ZR and Sun ZH: Tetrahydrocurcumin and octahydrocurcumin, the primary and final hydrogenated metabolites of curcumin, possess superior hepatic-protective effect against acetaminophen-induced liver injury: Role of CYP2E1 and Keap1-Nrf2 pathway. Food Chem Toxicol 123: 349-362, 2019.
35. Pop C, Berce C, Ghibu S, Scurtu I, Soriţău O, Login C, Kiss B, Ştefan MG, Fizeşan I, Silaghi H, *et al*: Effects of *Lycium barbarum* L. polysaccharides on inflammation and oxidative stress markers in a pressure overload-induced heart failure rat model. Molecules 25: 466, 2020.
36. Pan H, Shi Z, Yang TG, Yu LM and Ai-Li Xu AL: The protective effects of *Lycium barbarum* polysaccharides on retinal neurons in diabetic rats and its mechanism. Zhongguo Ying Yong Sheng Li Xue Za Zhi 35: 55-59, 2019 (In Chinese).
37. Varoni MV, Pasciu V, Gadau SD, Baralla E, Serra E, Palomba D and Demontis MP: Possible antioxidant effect of *Lycium barbarum* polysaccharides on hepatic cadmium-induced oxidative stress in rats. Environ Sci Pollut Res Int 24: 2946-2955, 2017.
38. Chen Y, Zeng M, Zhang Y, Guo H, Ding W and Sun T: Nlrp3 deficiency alleviates angiotensin II-induced cardiomyopathy by inhibiting mitochondrial dysfunction. Oxid Med Cell Longev 2021: 6679100, 2021.
39. Kim HJ, Sujiwo J, Kim HJ and Jang A: Effects of dipping chicken breast meat inoculated with Listeria monocytogenes in lyophilized scallion, garlic, and kiwi extracts on its physicochemical quality. Food Sci Anim Resour 39: 418-429, 2019.
40. Lee SY and Hur SJ: Effect of treatment with peptide extract from beef myofibrillar protein on oxidative stress in the brains of spontaneously hypertensive rats. Foods 8: 455, 2019.
41. El-Saka MH, Madi NM, Ibrahim RR, Alghazaly GM, Elshwaikh S and El-Bermawy M: The ameliorative effect of angiotensin 1-7 on experimentally induced-preeclampsia in rats: Targeting the role of peroxisome proliferator-activated receptors gamma expression and asymmetric dimethylarginine. Arch Biochem Biophys 671: 123-129, 2019.
42. Qin F, Xu MX, Wang ZW, Han ZN, Dong YN and Zhao JX: Effect of aerobic exercise and different levels of fine particulate matter (pM2.5) on pulmonary response in Wistar rats. Life Sci 254: 117355, 2020.
43. Mohammadjafari H, Arazi H, Nemati N, Bagherpoor T and Suzuki K: Acute effects of resistance exercise and the use of GH or IGF-1 hormones on oxidative stress and antioxidant markers in bodybuilders. Antioxidants 8: 587, 2019.
44. Zhou L, Wu CQ, Luo YW, Liao MY and Sun ZY: Studies on the characteristics and mechanisms of testicular toxicity induced by hydroxyurea. Toxicol Mech Methods 25: 396-401, 2015.
45. Estaquier J, Vallette F, Vayssiere JL and Mignotte B: The mitochondrial pathways of apoptosis. Adv Exp Med Biol 942: 157-183, 2012.
46. Hockenbery D, Nuñez G, Milliman C, Schreiber RD and Korsmeyer SJ: Bcl-2 is an inner mitochondrial membrane protein that blocks programmed cell death. Nature 348: 334-336, 1990.
47. Chiaramonte M, Inguglia L, Vazzana M, Deidun A and Arizza V: Stress and immune response to bacterial LPS in the sea urchin Paracentrotus lividus (Lamarck, 1816). Fish Shellfish Immunol 92: 384-394, 2019.
48. Bao C, Yang Z, Li Q, Cai Q, Li H and Shu B: Aerobic endurance exercise ameliorates renal vascular sclerosis in aged mice by regulating PI3K/AKT/mTOR signaling pathway. DNA Cell Biol 39: 310-320, 2020.
49. Teixeira GR, Mendes LO, Veras AS, Thorpe HH, Fávaro WJ, de Almeida Chuffa LG, Pinheiro PF and Martinez FE: Physical resistance training-induced changes in lipids metabolism pathways and apoptosis in prostate. Lipids Health Dis 19: 14, 2020.
50. Qie T, Xu P, Zhang BX and Cao XB: The effects of salidroside on the apoptosis pathway of myocardial cells in acute exhausted rats. Zhongguo Ying Yong Sheng Li Xue Za Zhi 35: 376-380, 2019 (In Chinese).
51. Zhang H, Liu M, Zhang Y and Li X: Trimetazidine attenuates exhaustive exercise-induced myocardial injury in rats via regulation of the Nrf2/NF-κB signaling pathway. Front Pharmacol 10: 175, 2019.
52. Wei Z, Cheng C, Zhou S, Chen C, Yu C, Lv N, Ji P, Wu X, Ma T, Cheng H, *et al*: Rosmarinic acid prevents refractory bacterial pneumonia through regulating Keap1/Nrf2-mediated autophagic pathway and mitochondrial oxidative stress.Free Radic Biol Med 168: 247-257, 2021.
53. Peng Z, Shu B, Zhang Y and Wang M: Endothelial response to pathophysiological stress. Arterioscler Thromb Vasc Biol 39: e233-e243, 2019.